# ARTICLE

OPEN

Impact of orbitally-driven seasonal insolation changes on Afro-Asian summer monsoons through the Holocene

Chi-Hua Wu [ID] [1✉] & Pei-Chia Tsai[1]

Understanding what drives a shift of the Afro–Asian summer monsoons from the continents to oceanic regions provides valuable insight into climate dynamics, changes, and modeling. Here we use data–model synthesis to focus on the differential seasonal responses of solar insolation and monsoons to orbital changes in the Holocene. We observe coordinated and stepwise seasonal evolution of summer monsoons across the mid-Holocene, suggesting the strengthening of the midlatitude jet stream as a bridge in the upper troposphere. Prior to the mid-Holocene, insolation had decreased considerably in early summer; the continental monsoons migrated southeastward, which corresponded to a more pronounced rainy season in coastal East Asia. In late summer, insolation did not decrease until the mid-Holocene. The continued weakening of the continental monsoons, combined with weakened insolation, rapidly enhanced the intrinsic dynamics over East Asia–Western North Pacific and accelerated a large-scale migration of the monsoon, suggesting orbital control of seasonal diversity.

[1] Research Center for Environmental Changes, Academia Sinica, Taipei, Taiwan. ✉email: chhwu@gate.sinica.edu.tw

Presently, the Afro–Asian summer monsoons have distinct timing onsets with a large range from late May to late July[1,2], following seasonal evolution of solar insolation and the mechanistic connection of the monsoons. Generally, interior heating drives the summer monsoons over South and East Asia in late spring to early summer, characterized by an inland or highland control of the monsoon. The evolution of the Western North Pacific (WNP) high and East Asian monsoon can be identical to the advancement of the South Asian monsoon, and the upper tropospheric circulation can be considered as a bridge connecting the monsoons[3]. In late July, the atmospheric circulation and precipitation enter another monsoon phase across West Africa, South Asia, and East Asia–WNP, corresponding to the development of the subtropical and oceanic monsoons[1]. In view of the seasonal variation of the upper tropospheric intercontinental anticyclone (with its center on South Asia, also recognized as the South Asian high[4]), which follows and influences underlying summer monsoon advancement, we may consider the Afro–Asian monsoon circulation as a system; also, the monsoonal climatology can be comparable between early summer and late summer, as the periods 15 May–15 June and August compared in this study. To explore what drives a shift of the Afro–Asian summer monsoons from the continents to oceanic regions (i.e., a comparison between early and late summer), we investigated the asynchronous Holocene evolution of the monsoons and focused on whether the seasonal differences in insolation between early and late summer would cause shifting patterns of the monsoons.

In the early Holocene, higher northern hemisphere summer insolation driven by the precession minimum and high obliquity enhanced and shifted continental monsoons farther norward over the Afro–Asian region[5–8], and correspondingly, the WNP high was stronger and expanded westward, suppressing the WNP monsoon trough[9]. In response to the reduction in northern hemisphere summer insolation due to orbital forcing, the Afro–Asian monsoon circulation weakened and migrated southeastward during the Holocene[10]; the monsoons were enhanced over subtropical and oceanic regions, suggesting that continental confinement with inland or highland origins was no longer typical of summer monsoons. As will be shown in this study, the orbitally-enhanced subtropical and oceanic monsoons would be seasonal. However, few studies have focused on differential responses of a monsoon system to seasonal orbital forcing on insolation changes[11].

The mechanistic connection of the monsoons has been considered in some of the leads and lags between insolation and various monsoon proxies[12–15]. In addition, studies suggest that oceanic contributions[16–18] and the interconnected nature of monsoons could be responsible for the major and potentially abrupt migration of the monsoons[10,19]. Related studies have focused on a see-saw relationship of the East Asian–Australian summer monsoon in the Holocene[20] and Saharan desertification[7,21]. According to Wu, et al.[9], in the early Holocene, the subtropical and oceanic monsoons were suppressed because of the synchronous strengthening of the continental monsoons and the WNP high, while the effect of the midlatitude circulation changes on the WNP monsoon was weak. The development and even formation of the subtropical and oceanic monsoons, involving the seasonal intrinsic dynamics over East Asia–WNP, might shed light on the rapid shift of large-scale monsoon patterns in the Holocene. It further motivated this study to investigate whether the strengthening of the oceanic monsoons contributed to the abrupt monsoon circulation change.

Results

Asynchronous seasonal and regional changes. Research has suggested that the early-to-mid-Holocene monsoons intensified and shifted northward over West Africa and Asia compared with their present-day conditions[7,10,17]. Proxy data have further suggested asynchronous pattern shifts in precipitation around the mid-Holocene. As the cave and marine core oxygen isotopes in Fig. 1 indicate (see the "Materials and methods" section for calculation of the trend, and Supplementary Tables 1–2 and Supplementary Fig. 1 for further details of the 14 proxy datasets used in this study), the climate was getting drier across 7 ka before present (BP) (Fig. 1c, d) over the Arabian Peninsula, the south of the Tibetan Plateau, and part of Northeastern Asia, apparently following the southward retreat of the monsoons. In contrast to the land regions that became drier, coastal East Asia throughout 7 ka BP and the South China Sea and subtropical WNP throughout 5 ka BP (Fig. 1e–f) became wetter. The climate modeling results, illustrated also in Fig. 1, suggested that the regional precipitation response to orbital changes, in particular over East Asia–WNP, may be related to the seasonal insolation changes between early and late summer.

Throughout 7 ka BP, when the dry tendency expanded southward over the Arabian Peninsula, south of the Tibetan Plateau, and Korea, the wetting trend of the oxygen isotopes was considerable over India and subtropical East Asia. This is closely related to the strengthening and even formation of the present style of the early Asian summer monsoon in early summer (15 May–15 June), as characterized by the Meiyu–Baiu season and the Bay of Bengal monsoon (increase in precipitation and intensification of cyclonic/negative streamfunction in the lower troposphere, Fig. 1a, c). By contrast, throughout 5 ka BP, the wetting trend over the South China Sea and subtropical WNP can be attributed to the weakening of the WNP high in early summer (anomalously cyclonic streamfunction, Fig. 1e) and the strengthening of the WNP monsoon trough in August (Fig. 1f). The climate modeling results suggested that the orbitally driven changes in the monsoons may vary by season.

To explore whether the difference in dynamical response between early summer and late summer, including the position of the WNP high and monsoon–midlatitude relationship in particular, would contribute to the asynchronous evolution of monsoons, we separately applied empirical orthogonal function (EOF) analysis on precipitation and dynamical fields in the lower and upper troposphere in 15 May–15 June and August (Fig. 2). The results suggested that major changes during the Holocene (11 ka BP to the present day) occurred before 4 ka BP in early summer (Fig. 2d) and after 7 ka BP in late summer (Fig. 2h). A change opposite to that seen in the early-summer evolution in the early-to-mid Holocene may have occurred since 4 ka BP (see below).

In the early and middle Holocene (11–4 ka BP), with respect to the early-summer monsoons, precipitation increased over the northern Arabian Sea, Bay of Bengal, and coastal East Asia, including the south of Japan, whereas it decreased over West Africa (Fig. 2a). At the same time that the precipitation changes occurred, anomalous anticyclonic/positive streamfunctions were visible over North and West Africa, the Arabian Peninsula, and West and central Asia, corresponding to the reduced precipitation in the Sahel and Middle East as well as a retreat of the South Asian summer monsoon (Fig. 2b). By contrast, anomalous cyclonic streamfunctions occurred over South Asia and East Asia–WNP, implying an increase in intensity of subtropical monsoons (closely related to the position of the present-day early-summer monsoons) and weakening and eastward retreat of the WNP high. In the upper troposphere, the westerly jet stream shifted southward, strengthened over subtropical regions, and exhibited a southwest–northeast tilt (Fig. 2c), corresponding to the large-scale contrast in lower tropospheric streamfunctions. The early-summer monsoon changes can be clearly identified prior to and around the mid-Holocene.
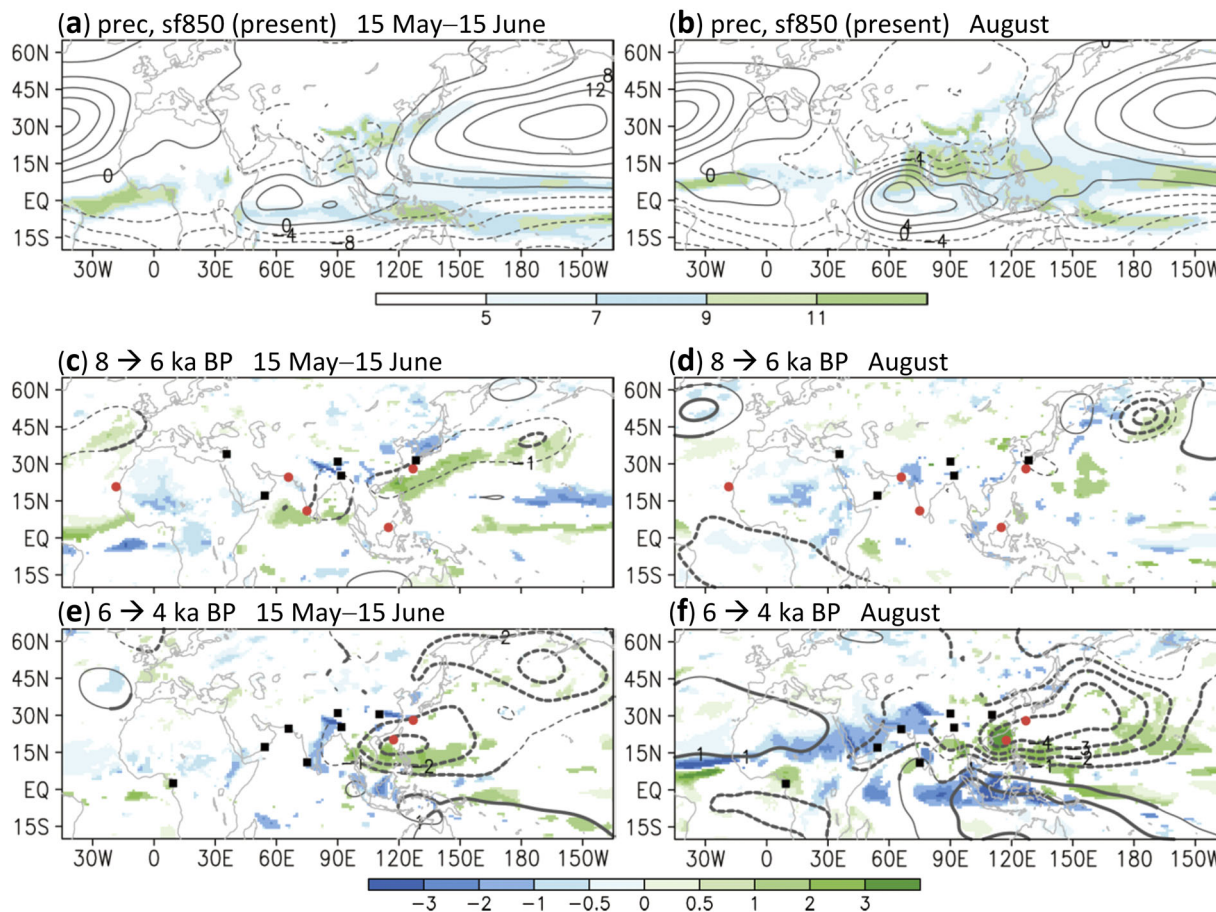
Fig. 1 Pattern shifts in data model synthesis. Simulated precipitation (shaded, mm day^{-1}) and streamfunction at 850 hPa (contours, 10^6 m^2 s^{-1}) in **a** 15 May–15 June and **b** August in the present. **c**, **d** Changes in simulated precipitation and the 850-hPa streamfunction from 8 ka BP to 6 ka BP in **c** 15 May–15 June and **d** August. **e**, **f** Same as **c**, **d** except for 6 ka BP to 4 ka BP. The thick contour lines denote differences in streamfunction with a confidence level of 90% (Student's t-test). Only the differences in precipitation with a confidence level of 90% are shown. Black squares/red dots denote the area getting drier/wetter across **c**, **d** 7 ka BP and **e**, **f** 5 ka BP.

Regarding the monsoons in late summer, with prominent changes during the mid-Holocene (6–4 ka BP), precipitation decreased over Africa, the southern Tibetan Plateau, and the Maritime Continent and increased over subtropical Asia and the WNP (Fig. 2e). The reduced precipitation in the Sahel and the retreat of the WNP high remained considerable (Fig. 2f). Differing from the anticyclonic streamfunction anomalies over West and central Asia (40°E–100°E) in early summer, the streamfunction in late summer exhibited a cyclonic anomaly over the region. In the upper troposphere, the westerly jet stream increased markedly over East Asia–WNP (Fig. 2g), corresponding to a sizable change in the lower tropospheric streamfunctions. As a major dynamic factor of the subtropical monsoons, the low-level westerly flow weakened over Africa and strengthened over the Indian Ocean and WNP (refer to Fig. 4d–f). The changes in oceanic monsoons can be clearly identified in the mid-Holocene, which critically brought the broad-scale and seasonal monsoon pattern closer to its present-day condition.

Monsoon dynamics, such as the strength of the monsoon flow over Africa, South Asia, and East Asia, consistently reveal a seasonal contrast in the Holocene evolution. A change occurred in the continental monsoons in early summer prior to the mid-Holocene, followed by a comprehensive (including late-summer monsoons) and even pronounced change in larger-scale circulation in the mid-Holocene. Associated with the seasonally lagged Holocene change, the difference between late summer and early

summer was most pronounced around the mid-Holocene (Supplementary Fig. 2).

Orbitally-driven seasonal insolation changes. Because perihelion occurred in July in the early Holocene and shifted to late August by 6 ka BP[16], the solar insolation changes could be seasonal. Compared with the early-Holocene state at 11 ka BP, the decrease in northern hemisphere insolation has occurred and intensified in early summer since the early Holocene, and the insolation change is more apparent prior to than after 4 ka BP (Fig. 3). In late summer, the decrease in insolation occurred a few thousand years later. As shown in Fig. 3b, the insolation in August along 30°N mostly increased prior to approximately 7 ka BP. It appears that the contrasting seasonal insolation changes have given support to the major changes in the atmospheric circulation and precipitation as the EOF analyses indicate. A further analysis has confirmed that the changes in atmospheric heating and geopotential heights, particularly those associated with continental monsoons (Africa and South Asia), followed well after the seasonal insolation changes (Supplementary Fig. 3).

The changes in the insolation between seasons can be also considerable during the Holocene. At 11 ka BP and 30°N, the insolation was approximately 50 W m^{-2} higher during early summer than late summer (i.e., 15 May–15 June versus August, Fig. 3b). In the early Holocene between 11 ka BP and 7 ka BP, the
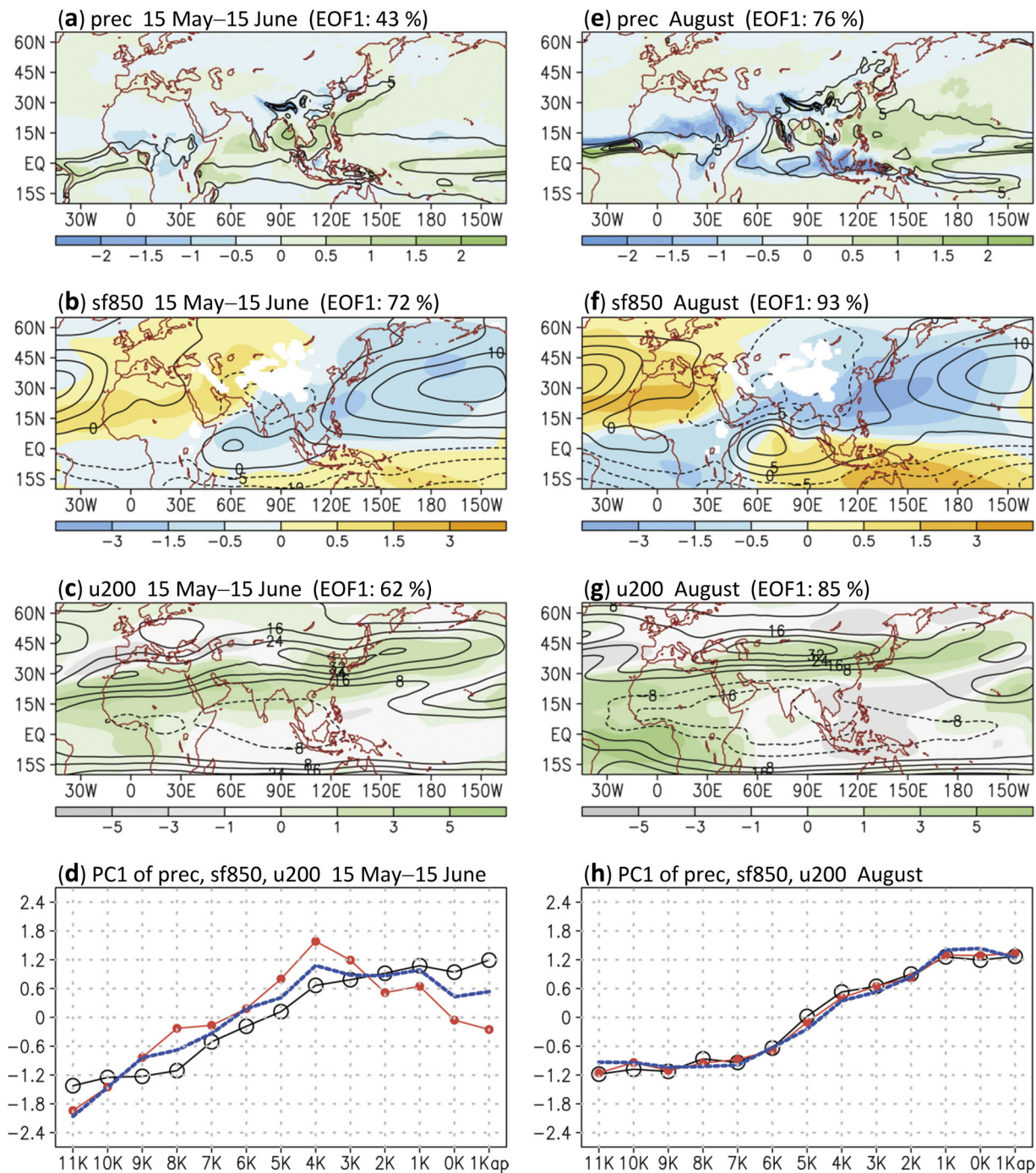
Fig. 2 Holocene changes in dynamic fields. The EOF1 of **a** precipitation, **b** streamfunction at 850 hPa, and **c** zonal winds at 200 hPa in 15 May–15 June (shaded) from 11 ka BP (11 K) across the present day (0 K) to 1 ka after the present (1 Kap); contour lines denote the corresponding fields in the present day (unit of precipitation is mm day^{-1}, unit of streamfunction is 10^6 m^2 s^{-1}, and unit of zonal wind is m s^{-1}); the percentage of total variance explained by EOF is also provided. **d** Corresponding principal components (precipitation: black circles; streamfunction: red dots; zonal winds: blue). **e–h** Same as **a–d** except for August.

seasonal variation of insolation diminished rapidly associated with the contrasting insolation changes (i.e., the decrease in early summer and the increase in late summer). The subtropical insolation contrast in early relative to late summer reached a quasi-equilibrium state with approximately 15 W m^{-2} in difference around the mid-Holocene, corresponding to a synchronously seasonal decrease in insolation. During the late Holocene, because the insolation continued to decrease in late summer and re-increased in early summer, the seasonal insolation variation re-

increased. Associated with seasonal insolation changes between early and late summer, the asynchronous evolution of the summer monsoons during the Holocene might have been influenced by the orbitally-driven variation on the millennium scale, as the millennial-scale evolution of lower tropospheric streamfunction in Fig. 3c indicates (i.e., the WNP high changes in early summer and the weakening of African monsoon and deepening of the WNP monsoon trough in late summer). Meanwhile, the increased seasonal contrast in insolation (in different months) might
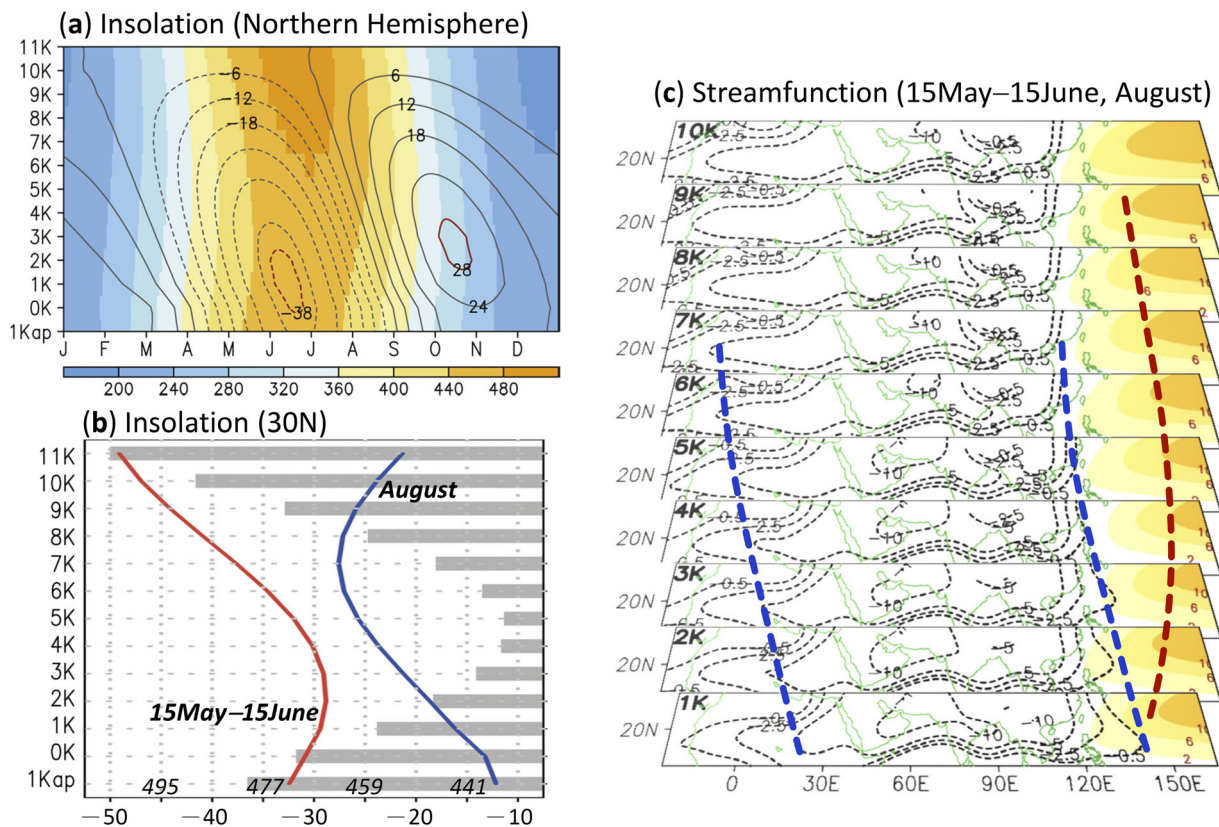
Fig. 3 Insolation changes. a Annual variation in the Northern Hemisphere insolation from 11 ka BP (11 K) to 1 ka after the present (1Kap) (shaded, unit: W m^{-2}); contours denote that the insolation in 11 ka BP is subtracted. **b** Same as **a** except for averaged in 15 May–15 June (red line), August (blue line), and difference in between (gray bars) along 30°N. (**c**) Evolution of streamfunction at 850 hPa (unit: 10^6 m^2 s^{-1}) in 15 May–15 June (shaded, only for positive values) and August (contours, only for negative values) from 10 ka BP to 1 ka BP.

substantially affect the seasonal diversity of the monsoons over West Africa, South Asia, and East Asia–WNP. A suggestion might be that the present-day monsoon phase transition in late July is inevitable because the continental monsoon no longer has dominant control of large-scale circulation.

Coordinated Afro-Asian monsoon evolution in the mid-Holocene. With respect to the large-scale Holocene evolution, major changes may have occurred in early summer prior to approximately 4 ka BP and in late summer after approximately 7 ka BP. To further explore regional differences in the Holocene evolution, we analyzed the leading EOF analysis results of zonal winds at 850 hPa and precipitation (Fig. 4) and focused on the monsoon subregions, including Africa (20°W–20°E), the Arabian Sea (50°E–70°E), and East Asia–WNP (110°E–140°E). Overall, the major summer monsoon changes can be clearly identified following the paradigm of a southeastward retreat of the monsoon circulation.

In Africa (Fig. 4a, d), the lower tropospheric westerlies (850 hPa) and precipitation consistently weakened over the region approximately north of 10°N in June–September. Over the region covering the Arabian Sea (Fig. 4b, e), where the seasonal advancement of the Somali jet stream sometimes has dominant control, the westerlies in the region north of 15°N exhibited the largest decrease in June–July and the largest decrease in precipitation in July–September. As demonstrated by the strengthening of the westerlies over the region between 15°N and the equator (Fig. 4e), the Somali jet stream was confined to the equator, corresponding to the southward shift of the monsoon position. The first principal component (PC1) of the analyzed

fields over these two regions suggests a gradual evolution of the monsoons during the Holocene (Fig. 4j, k).

Over the East Asia–WNP region (Fig. 4c, f), a southward retreat of Meiyu precipitation and the wind band occurred in May–June, and the westerlies and precipitation in the tropical WNP (5°N–25°N) increased in July–September. Intriguingly, the PC1 of the East Asia–WNP region suggests a rapid change between 6 and 4 ka BP (Fig. 4l). The enhancement and even formation of the oceanic monsoon was likely a major contributor to the large-scale and abrupt change in the mid-Holocene.

The midlatitude westerly jet stream can be a major dynamic factor in the monsoon changes because of its strength and position, whether on a synoptic or planetary scale[22,23]. Overall, the change in large-scale circulation prior to the mid-Holocene was characterized by a southeastward migration, and the strengthening of the westerly jet stream had substantial effects on enhancing the Meiyu–Baiu season (See Supplementary Fig. 4 for further discussion). Originally because of the seasonal contrast in orbitally driven insolation changes, the monsoons gradually changed in early summer prior to the mid-Holocene, characterized by a southeastward migration of continental monsoons. A drastic change in large-scale circulation occurred until the mid-Holocene, apparently with collaborated evolution of monsoons in Africa, South Asia, and East Asia–WNP. The vertical circulation coupling over East Asia–WNP, as characterized by the upper tropospheric jet stream and lower tropospheric WNP high, might contribute to accelerating mid-Holocene climate change.

A two-step migration of the Afro–Asian circulation in the mid-Holocene, involving coordinated evolution of the subtropical summer monsoons, is therefore suggested: (a) Prior to the mid-Holocene, the continental monsoons had been shifting
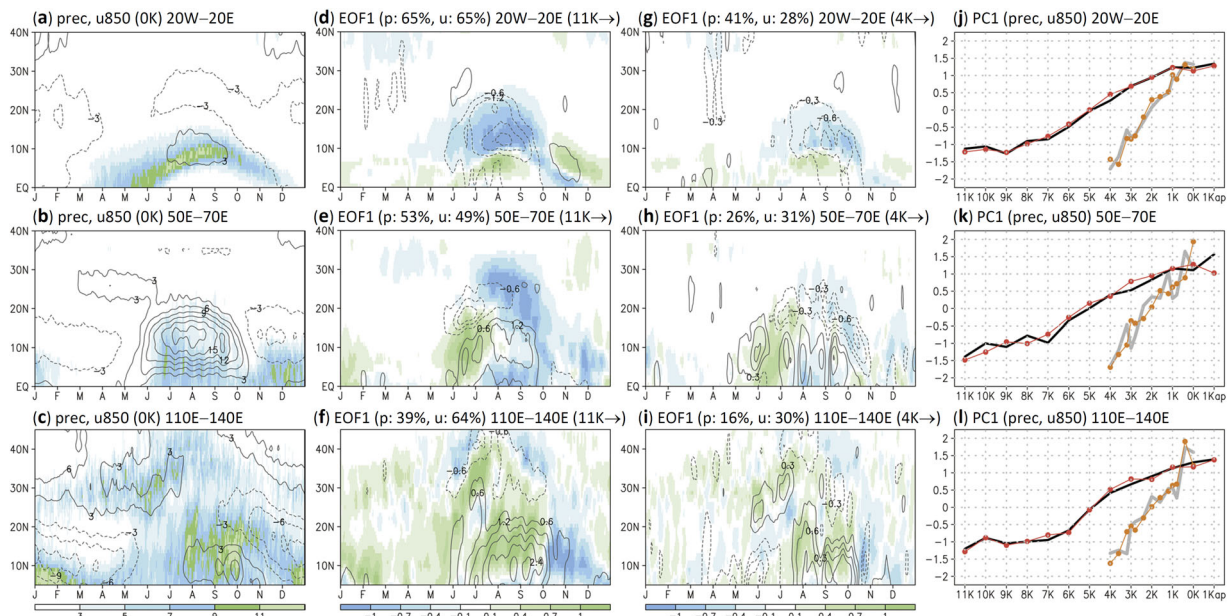
Fig. 4 Annual variation in monsoon regions. Annual variation in precipitation (shaded, unit: mm day^{-1}) and zonal winds at 850 hPa (contours, unit: m s^{-1}) in **a** 20°W–20°E, **b** 50°E–70°E, and **c** 110°E–140°E at the present (0 K). **d–f** The EOF1 of precipitation (shaded) and the 850-hPa zonal winds (contours) in 11 ka BP (11 K)–1 ka after present (1Kap); the percentage of total variance explained by EOF is also provided. **g–i** Same as **d–f** except for 4–0 ka BP. **j–l** The corresponding PC1 of precipitation (black and gray) and the 850-hPa zonal winds (red and orange).

southeastward and weakening to a certain extent, which was visible in early summer and could be attributed to the orbitally driven reduction in insolation. (b) The orbitally reduced insolation persisted and intensified in late summer across the mid-Holocene. This favored the sideways expansion of the upper tropospheric intercontinental anticyclone, which is associated with an enhancement and even formation of the intrinsic dynamics in East Asia–WNP, including the Pacific–Japan (PJ) pattern[24] with a tropical oceanic origin and a strong midlatitude connection[25].

Seasonal evolution in the late Holocene. In the late Holocene, the early-summer insolation change was much smaller than that in the early and middle Holocene and the insolation began to increase toward the present day, whereas the late-summer insolation continued to decrease (Fig. 3). Figure 2 shows a secondary signal in early summer since 4 ka BP, which might imply reversed shifting patterns during the late Holocene, compared with the pattern shifts in the early-to-mid Holocene. To explore the changes in the late Holocene, we conducted extra time-slicing simulations from 4 ka BP to the present day (see "Materials and methods" section). Overall, the Pacific high restrengthened and expanded westward in the late Holocene, corresponding to a weakening of the upper-level westerly jet stream in the subtropical Asia and a reduction in monsoon precipitation in coastal South and East Asia. Meanwhile, nearly no changes occurred in precipitation and low-level streamfunction in Africa (See Supplementary Fig. 5 for further discussion). During the late Holocene, the atmospheric conditions changed only partly over Afro–Asia in early summer opposite to the changes during the early-to-mid-Holocene.

The leading EOF analysis results of the monsoon subregions show the contrasting changes more clearly in early versus late summer and in the late versus the whole Holocene (compared Fig. 4d–f, g–i). In the late Holocene since 4 ka BP, the changes in late summer were considerable and mostly consistent with the mid-Holocene changes. By contrast, in early summer, the changes in the late Holocene disappeared in Africa and occurred in opposite signal in the Arabian Sea and East Asia–WNP. We recall attention to the weakening of the early-summer continental monsoons during the early-to-mid Holocene, which could be a precursor of the broad-scale monsoon changes. Partly due to a relatively low insolation in the late Holocene compared to previous times, the subtropical and oceanic monsoons were continuously enhanced, in contrast to the re-strengthening of the early-summer monsoons over South and East Asia.

Discussion
In this study, the strengthening and southward shift of the midlatitude westerly jet stream is considered a major dynamic factor in the coordinated evolution of the Afro–Asian summer monsoons in the Holocene. Furthermore, the coupling between the upper tropospheric westerlies and the underlying monsoon circulation, partly associated with an enlarged perturbation of the jet stream, could be suggested to be a connection between the monsoons. A similar emphasis on the role of a changing jet stream may promote understanding of decadal changes in monsoons. A recent modulation of the Silk Road pattern[25] and frequency in the double-jet phenomenon[26] were attributed to amplified summer warming on the Eurasian continent[27,28]. A westward shift and advanced Asian summer monsoon have been further suggested as reasons for the recent increase in temperature[29,30].

Studies have also suggested that dynamic mechanisms involving the influence of the vegetation–atmosphere–ocean interaction[31–33] could result in the phase transition from the Green Sahara[34] in the early-to-mid-Holocene to its present-day condition. Inflow of low-moisture static energy air from the ocean or poleward region as a result of a ventilation mechanism has been further suggested as a major process in setting the northern boundary for the African monsoon[35]. Following a Gill–Matsuno-type mechanism[36,37], the influence of the tropical Atlantic on the monsoons over Africa and South Asia has also been considerable[38]. Large-scale control and a remote connection to changes in other monsoons may reasonably be related to the stepwise monsoon evolution in a region. Decadal drying of Sahel summer

precipitation was attributed to increased summer monsoons over South Asia and the WNP[39], implying a connection between the monsoons. Driven by early-Holocene orbital forcing, with extremely high summer insolation, the enhanced African monsoon corresponded to a strengthened and westward expansion of the WNP high, a weakened midlatitude westerly jet stream, and weakened subtropical Asian monsoons. Thus, the WNP monsoon trough in the lower troposphere might disappear[9]. Earlier modeling results further illustrated that oceanic feedback in the mid-Holocene strengthened the African monsoon but weakened the Asian monsoon[16]. The Holocene evolution of the monsoons with inland or highland origins and the monsoons with subtropical and oceanic origins, with opposite signals, are likely correlated.

Besides, the differential response of land and ocean to orbital forcing was emphasized, and suggested as a controlling mechanism of monsoon intensity when the amplitude of solar forcing falls below the threshold level[40]. We have further examined the orbitally driven Holocene changes in surface temperature by conducting EOF analysis on temperatures over land (globally in 60°S–60°N) and distinct oceans, including the tropical Indian Ocean (20°S–20°N), North Atlantic Ocean (0°–60°N), and the WNP (0°–40°N) (Supplementary Fig. 6). The abrupt changes during the mid-Holocene could only be identified as considerable in the WNP region, and were characterized partly by a reduction in sea surface temperature in late summer. Thus, regarding the abrupt formation of the Holocene PJ pattern in late summer, sea surface temperature might have played a passive role. However, partly due to the focus on the Afro–Asian monsoons, we may have not fully explored the shifting patterns including the modeling circulation changes across the equator and over the North Atlantic Ocean; also, other paleoclimate forcings and their potential impact on monsoons have not been investigated. Further simulations with deep ocean circulation and including other paleoclimate forcing would provide valuable information.

Moreover, compared to that in the early and middle Holocene, the change in insolation and atmospheric circulation in many aspects was smaller in the late Holocene. Unlike an accelerated decrease in obliquity, precession reached a minimum around 1 ka BP and had much smaller changes in the late than middle Holocene. Our simulations, by comparing previous modeling results focusing also on orbital impact[8,41], may have confirmed the obliquity's contribution in the late Holocene only in late summer (Supplementary Fig. 7). It is worth of further investigation on how the precession versus obliquity affects monsoons in the late Holocene. Understanding of the role of decreasing obliquity in the late Holocene might be able to further provide insights into orbital forcing on a projected future climate change.

Methods

We collected 14 proxy records with relatively high temporal resolution in the Holocene (11–0 ka BP) across the Afro–Asia region. Proxy data included cave and marine core oxygen isotopes, which were measured for precipitation and hydro-climate and downloaded from the paleoclimatology data website of the National Oceanic and Atmospheric Administration (NOAA). We detected a wetting or drying trend during 2000 consecutive years, as identified by 1000-year averaged oxygen isotopes between a given reference time. For example, the trend throughout 5 ka BP was calculated as the average of 4–5 ka BP minus the average of 5–6 ka BP. The time-slicing simulations between 4 and 6 ka BP were compared with the trend of proxy records across 5 ka BP. We further calculated the standard deviation by using available data of a proxy record in 11–0 ka BP. Only the trends with a difference greater than 0.3-times the standard deviation (the thresholds of 0.2 and 0.4 did not have a significant modulating effect on the results) for 2000 consecutive years are shown in Fig. 1 (refer to Fig. 1a and Supplementary Table 1; Supplementary Fig. 1 for further details of the used records).

To explore atmospheric response to orbital changes during the Holocene, we used the Community Atmospheric Model (CAM) version 5.1 of the National Center for Atmospheric Research (NCAR) and the slab ocean model (SOM) (http://www.cesm.ucar.edu). CAM and SOM simulations were integrated using the finite volume dynamical core with 1° horizontal resolution and 30 vertical levels in

the CAM[42]. Studies have shown that the combination of CAM and SOM reflects realistic climatological seasonality over the Asian summer monsoon region[9,23]. A total of 21 time-slicing experimental simulations (from the early Holocene across the present day to 1 ka after the present) were performed; in addition to the 13 simulations from 11 ka BP to 1 ka AP with interval of 1000 years (refer to Supplementary Table 2 for detailed orbital parameters), extra eight simulations at the orbital conditions of 3.6, 3.2, 2.8, 2.4, 1.6, 1.2, 0.8, and 0.4 ka BP were performed for higher resolution in the late Holocene. The boundary and initial conditions of the simulations were taken from the Community Earth System Model (CESM) preindustrial control experiment[43]. The model was integrated for 40 years, and outputs for years 21–40 were used to form the climatology. Inevitably, our time-slicing experimental simulations did not include deep oceanic circulation changes and feedbacks between vegetation and the atmosphere, which could be a major source of uncertainty in a comparison between paleoclimate data and modeling.

Data availability

References

1. Wu, C.-H., Wang, S. Y. S. & Hsu, H.-H. Large-scale control of the Arabian Sea monsoon inversion in August. *Clim. Dyn.* **51**, 2581–2592 (2017).
2. Wu, C.-H. & Hsu, H.-H. Role of the Indochina Peninsula narrow mountains in modulating the east asian–western north Pacific summer monsoon. *J. Clim.* **29**, 4445–4459 (2016).
3. Wu, C.-H., Chou, M.-D. & Fong, Y.-H. Impact of the Himalayas on the Meiyu–Baiu migration. *Clim. Dyn.* **50**, 1307–1319 (2017).
4. Wu, G. X. et al. Tibetan Plateau climate dynamics: recent research progress and outlook. *Natl Sci. Rev.* **2**, 100–116 (2015).
5. Rossignol-Strick, M. African monsoons, an immediate climate response to orbital insolation. *Nature* **304**, 46–49 (1983).
6. Kutzbach, J. E. Monsoon climate of the early Holocene: climate experiment with the Earth's orbital parameters for 9000 years ago. *Science* **214**, 59–61 (1981).
7. Crucifix, M., Loutre, M. F., Tulkens, P., Fichefet, T. & Berger, A. Climate evolution during the Holocene: a study with an Earth system model of intermediate complexity. *Clim. Dyn.* **19**, 43–60 (2002).
8. Wu, C. H., Lee, S. Y. & Chiang, J. C. H. Relative influence of precession and obliquity in the early Holocene: topographic modulation of subtropical seasonality during the Asian summer monsoon. *Quat. Sci. Rev.* **191**, 238–255 (2018).
9. Wu, C.-H., Chiang, J. C. H., Hsu, H.-H. & Lee, S.-Y. Orbital control of the western North Pacific summer monsoon. *Clim. Dyn.* **46**, 897–911 (2015).
10. Fleitmann, D. et al. Holocene ITCZ and Indian monsoon dynamics recorded in stalagmites from Oman and Yemen (Socotra). *Quat. Sci. Rev.* **26**, 170–188 (2007).
11. Braconnot, P., Marzin, C., Gregoire, L., Mosquet, E. & Marti, O. Monsoon response to changes in Earth's orbital parameters: comparisons between simulations of the Eemian and of the Holocene. *Clim. Past* **4**, 281–294 (2008).
12. Wang, Y. B. et al. Coherent tropical-subtropical Holocene see-saw moisture patterns in the Eastern Hemisphere monsoon systems. *Quat. Sci. Rev.* **169**, 231–242 (2017).
13. Wang, Y. B., Liu, X. Q. & Herzschuh, U. Asynchronous evolution of the Indian and East Asian summer monsoon indicated by Holocene moisture patterns in monsoonal central Asia. *Earth Sci. Rev.* **103**, 135–153 (2010).
14. Zhang, X., Jin, L., Chen, J., Lu, H. & Chen, F. Lagged response of summer precipitation to insolation forcing on the northeastern Tibetan Plateau during the Holocene. *Clim. Dyn.* **50**, 3117–3129 (2017).
15. An, Z. S. et al. Asynchronous Holocene optimum of the East Asian monsoon. *Quat. Sci. Rev.* **19**, 743–762 (2000).
16. Liu, Z., Harrison, S. P., Kutzbach, J. & Otto-Bliesner, B. Global monsoons in the mid-Holocene and oceanic feedback. *Clim. Dyn.* **22**, 157–182 (2004).
17. Wang, Y. et al. The Holocene Asian monsoon: links to solar changes and North Atlantic climate. *Science* **308**, 854–857 (2005).
18. Gupta, A. K., Anderson, D. M. & Overpeck, J. T. Abrupt changes in the Asian southwest monsoon during the Holocene and their links to the North Atlantic Ocean. *Nature* **421**, 354–357 (2003).

19. deMenocal, P. et al. Abrupt onset and termination of the African humid period: rapid climate responses to gradual insolation forcing. *Quat. Sci. Rev.* **19**, 347–361 (2000).
20. Eroglu, D. et al. See-saw relationship of the Holocene East Asian-Australian summer monsoon. *Nat. Commun.* **7**, 12929 (2016).
21. Shanahan, T. M. et al. The time-transgressive termination of the African humid period. *Nat. Geosci.* **8**, 140–144 (2015).
22. Chen, F. H. et al. Westerlies Asia and monsoonal Asia: Spatiotemporal differences in climate change and possible mechanisms on decadal to sub-orbital timescales. *Earth Sci. Rev.* **192**, 337–354 (2019).
23. Chiang, J. C. H. et al. Role of seasonal transitions and westerly jets in East Asian paleoclimate. *Quat. Sci. Rev.* **108**, 111–129 (2015).
24. Nitta, T. Convective activities in the tropical Western Pacific and their impact on the northern-hemisphere summer circulation. *J. Meteorol. Soc. Jpn* **65**, 373–390 (1987).
25. Enomoto, T., Hoskins, B. J. & Matsuda, Y. The formation mechanism of the Bonin high in August. *Q. J. R. Meteorol. Soc.* **129**, 157–178 (2003).
26. He, Y. et al. Comparison of the effect of land-sea thermal contrast on interdecadal variations in winter and summer blockings. *Clim. Dyn.* **51**, 1275–1294 (2017).
27. Li, Y., Ding, Y. H. & Li, W. J. Interdecadal variability of the Afro-Asian summer monsoon system. *Adv. Atmos. Sci.* **34**, 833–846 (2017).
28. Hong, X., Riyu, L. & Shuanglin, L. Amplified summer warming in Europe–West Asia and Northeast Asia after the mid-1990s. *Environ. Res. Lett.* **12**, 094007 (2017).
29. Preethi, B., Mujumdar, M., Kripalani, R. H., Prabhu, A. & Krishnan, R. Recent trends and tele-connections among South and East Asian summer monsoons in a warming environment. *Clim. Dyn.* **48**, 2489–2505 (2016).
30. Kajikawa, Y., Yasunari, T., Yoshida, S. & Fujinami, H. Advanced Asian summer monsoon onset in recent decades. *Geophys. Res. Lett.* **39**, n/a–n/a (2012).
31. Ganopolski, A., Kubatzki, C., Claussen, M., Brovkin, V. V. & Petoukhov, V. V. The influence of vegetation-atmosphere-ocean interaction on climate during the mid-holocene. *Science* **280**, 1916–1919 (1998).
32. Rachmayani, R., Prange, M. & Schulz, M. North African vegetation–precipitation feedback in early and mid-Holocene climate simulations with CCSM3-DGVM. *Clim. Past* **11**, 175–185 (2015).
33. Kutzbach, J. E. & Liu, Z. Response of the African monsoon to orbital forcing and ocean feedbacks in the middle Holocene. *Science* **278**, 440–443 (1997).
34. Tierney, J. E., Pausata, F. S. & deMenocal, P. B. Rainfall regimes of the Green Sahara. *Sci. Adv.* **3**, e1601503 (2017).
35. Su, H. & Neelin, J. D. Dynamical mechanisms for African monsoon changes during the mid-Holocene. *J. Geophys. Res. Atmos.* **110**, D19 (2005).
36. Gill, A. E. Some simple solutions for heat-induced tropical circulation. *Quart. J. R. Meteorol. Soc.* **106**, 447–462 (1980).
37. Matsuno, T. Quasi-geostrophic motions in the equatorial area. *J. Meteorol. Soc. Jpn Ser. II* **44**, 25–43 (1966).
38. Kucharski, F. et al. A Gill-Matsuno-type mechanism explains the tropical Atlantic influence on African and Indian monsoon rainfall. *Quart. J. R. Meteorol. Soc.* **135**, 569–579 (2009).
39. He, S., Yang, S. & Li, Z. Influence of latent heating over the Asian and Western pacific monsoon region on Sahel summer rainfall. *Sci. Rep.* **7**, 7680 (2017).
40. Nakagawa, T. et al. Regulation of the monsoon climate by two different orbital rhythms and forcing mechanisms. *Geology* **36**, 491–494 (2008).
41. Wu, C. H. & Tsai, P. C. Obliquity-driven changes in East Asian seasonality. *Glob. Planet. Change* **189**, 103161 (2020).
42. Neale, R. B. et al. The mean climate of the community atmosphere model (CAM4) in forced SST and fully coupled experiments. *J. Clim.* **26**, 5150–5168 (2013).
43. Vertenstein, M. T. C., Middleton, A., Feddema, D. & Fischer, C. CESM1.0.3 User's Guide. Available at: http://www.cesm.ucar.edu/. (2010).

Author contributions
C.H.W. organized analyses, performed experimental simulations, and wrote manuscript. P.C.T. assisted data analyses and contributed to preparing data and figures.

Competing interests
The authors declare no competing interests.

Additional information
Supplementary information is available for this paper at https://doi.org/10.1038/s43247-020-00073-8.

Correspondence and requests for materials should be addressed to C.-H.W.

Reprints and permission information is available at http://www.nature.com/reprints

Publisher's note Springer Nature remains neutral with regard to jurisdictional claims in published maps and institutional affiliations.